Available online at www.sciencedirect.com
ScienceDirect
Optics and Lasers in Engineering 45 (2007) 373–379
OPTICS and LASERS in ENGINEERING

# Periodically poled lithium niobate structures grown by the off-center Czochralski technique for backward and forward second harmonic generation

N. Argiolas[a], M. Bazzan[a], E. Cattaruzza[a], A. Gasparini[a], P. Mazzoldi[a], C. Sada[a,*], A.D. Capobianco[b], E. Autizi[c], F.M. Pigozzo[d], A. Locatelli[e], L.C. Guarneri[e]

[a]*MATIS-INFM and Physics Department, Padova University, Via Marzolo 8, 35131 Padova, Italy*
[b]*INFM and DEI Department, Padova University, Via Gradenigo 6/b, 35131 Padova, Italy*
[c]*DEI Department, Padova University, Via Gradenigo 6/b, 35131 Padova, Italy*
[d]*DIEGM Department, Udine University, Via delle Scienze 208, 33100 Udine, Italy*
[e]*INFM and DEA Department, Brescia University, Via Branze 38, 25123 Brescia, Italy*

Available online 3 May 2006

**Abstract**

We report on the characterization of periodically poled lithium niobate structures grown by the off-center Czochralski technique with periods ranging between 2 and 10 μm. The domains distribution along the crystal was inspected by a profilometer scan after etching the structures and carrying a suitable data processing. The second harmonic generation efficiency was predicted by numerically integrating the governing equations through to a recently proposed nonlinear bidirectional beam propagation method. The numerical analysis pointed out the feasibility of the backward second harmonic generation in the sample with the shortest domain period. The predicted second harmonic generation efficiency was finally corrected considering the phase shifts induced in the second harmonic wave by the presence of different sized domains.


*Keywords:* Periodically poled lithium niobate; Crystal growth; Beam propagation method; Second harmonic generation

## 1. Introduction

Today efforts made in optoelectronics and photonics are mainly focused to develop faster, more efficient ways of acquiring, storing and transmitting information and, consequently, there is a drive to obtain better nonlinear materials. When second-order nonlinear effects are considered, however, efficient nonlinear interactions require that the phase matching conditions are fulfilled between two interacting waves. To this purpose, periodic structures have been widely used to overcome the dispersion of the refractive index. In particular, it has been demonstrated that an efficient second harmonic generation (SHG) can be achieved in periodically poled lithium niobate (PPLN) crystals via the quasi-phase matching (QPM) method [1]. Since QPM was first introduced, the attention was mostly concentrated on forward SHG, where a pump beam propagating in a second-order nonlinear medium can generate a second-harmonic (SH) beam propagating along the same direction. On the other hand, it was shown [2,3] that a backward (BW) SHG is possible. In this case a pump beam can generate a SH beam propagating along the opposite direction. There are certain potential advantages of BW SHG [4]. Among the most promising applications, we mention the remote sensing via SHG or optical parametric oscillation since the backward SH or parametric waves will follow the optical path and propagate back to the pump beam [5]. However, it was shown that for the first-order phase matching at a fundamental wavelength of 1.55 μm a period close to 0.178 μm is needed [6]. This fact can represent a strong limitation for the experimental techniques used to prepare PPLN structures. As a matter of fact, periodically poled structures are

*Corresponding author. Tel.: +39 049 8277037; fax: +39 49 8277 003.
*E-mail address:* sada@padova.infm.it (C. Sada).

0143-8166/$ - see front matter © 2006 Elsevier Ltd. All rights reserved.
doi:10.1016/j.optlaseng.2005.04.018

usually prepared by the electric-field poling technique by applying an electric field either during the material growth (about 0.4 V/cm) or after that, even at room temperature [7,8]. In this case, when small periods are required complications can arise from such very narrow electrode deposition. However, it was demonstrated that with the intentional displacement of the growth axis from the symmetry axis of the temperature field, periodic fluctuations of temperature occur leading to the periodic domains reversal [9]. The result is a PPLN structure ranging through the whole crystal, typically few centimeters long. This technique can be considered a suitable alternative to prepare tailored periodic structures. Up to our knowledge, the off-center Czochralski technique has not been tested to grow PPLN structures with period as short as required by the QPM condition for the BW SHG. Unfortunately during the PPLN growth imperfections in the structure periodicity can occur, such as random errors or periodic modulation in the domain width [10]. Depending on their magnitude, these imperfections lead to a reduction of the SHG efficiency and, therefore, should be deeply investigated. The control in the structure periodicity is one of the key points to optimize the device performances, especially when small periods are concerned. The aim of this work is to predict the SHG efficiency resulting by the propagation of the fundamental beam in "real", and therefore imperfect, PPLN samples in function of the process parameters. We intend to investigate the conditions needed to obtain an efficient SHG both in FW and BW configurations. For this reason, we adopt a numerical tool (a recently proposed nonlinear bidirectional beam propagation method, NL Bi BPM) to predict the amount of energy conversion in ideal PPLN structures. Subsequently we exploit the method of Fejer et al. to estimate the effect of border domain errors. To this goal we perform a map of the periodic domain structures using a standard profilometer after a chemical etching process. This analysis was carried out on PPLN samples with periods ranging between 2 and 10 μm.

## 2. Experimental

Periodically poled Er: $LiNbO_3$ single crystals were grown by the off-center Czochralski technique [9,11] starting from a $LiNbO_3$ melt containing 0.5–0.7 mol% of $Er_2O_3$. The growth conditions were chosen to tailor the PPLN periods, as reported in Table 1, ranging between 2 and 10 μm, respectively. In particular, the pulling rate $v_p$ was varied from 2 to 3 mm/h, the rotation rate ($\omega$) from 4 to 16.7 rpm while the off-center was ranged between 7 and 9 mm. The crystals containing the PPLN structure were cut to give Z-cut slices, polished and finally etched in an acid solution ($HF: HNO_3 = 1:2$ in volume) at 80 °C for about 3 min. As the etching rate is faster for a negative $-Z$ face than for a positive one (see Ref. [12]), etched domains with opposite polarization states result in a sequence of hole–peak–hole, respectively. Therefore, they can be easily identified by a profilometer scanning. The optimal etching conditions were chosen to avoid selective etching artifacts [13] due to the material lateral erosion arising whenever the etching process is long or the temperature is too high. This lateral etching introduces artifacts in the measure of the domain widths, the positive domains becoming smaller than the negative ones. In absence of the lateral etching, the positive and negative domains have the same width within experimental errors. We investigated the PPLN periodicity by mapping the etched surfaces using a Tencor profilometer (with lateral resolution equal to few nm and a depth resolution of about 1 nm). The scan was performed along the direction normal to the border domain with a scanning speed equal to 1 μm $s^{-1}$ and a sampling rate of 500 Hz. The measured scan is, however, the result of the "convolution" of the profilometer tip shape with the real pattern profile of the etched PPLN crystal. To obtain the real PPLN pattern a deconvolution procedure was applied, following the procedure described in Ref. [11]. In particular, the position of the border domain is obtained by analyzing the numerical derivative of the deconvoluted scanned profile. Since an edge corresponds to each border domain, the procedure allows to identify the edge position and returns (i) the domain wall location, and (ii) the domain width or period of the structure as a function of the position. Further details on the procedure used in the present work were reported in Ref. [11].

## 3. Results

In Fig. 1 we report the scan of the positive and negative domain widths across the Z-cut slices for crystals with off-center equal to 7 mm. Similar scans were performed on the other PPLN structures grown under the experimental conditions summarized in Table 1. The dips refer to the negative domains which, as previously mentioned, are etched faster than the positive ones. By processing the data

Table 1
Growth conditions of the PPLN structures. In the last two columns the PPLN period $\Lambda$ of the PPLN structures grown by the off-center Czochrlaski technique has been reported together with the corresponding experimental error

| Name | $Er_2O_3$ (mol%) | $v_p$ (mm/h) | $\omega$ (rpm) | off-center (mm) | $\Lambda$ (μm) | $\delta_\Lambda$ (μm) |
|---|---|---|---|---|---|---|
| PPLN1 | 0.7 | 2.0 | 16.7 | 9 | 2.14 | 0.16 |
| PPLN4 | 0.7 | 2.0 | 5.5 | 7 | 7.40 | 1.54 |
| PPLN5 | 0.5 | 2.0 | 4.0 | 7 | 9.96 | 1.46 |

given by the profilometer scan, it is possible to investigate the domain width distribution along the PPLN structure [10,11] and to highlight whether errors in the domain positions occur along the crystal. From the analysis of the scanning map (not reported) the domain width changes significantly along the whole crystal, i.e. from the shoulder to the bottom. In particular, during the Czochralski growth when the temperature decreases passing from the shoulder to the body of the boule, the domains width increases up to an almost constant value along the body. This analysis allows the identification of the best region where the domain width distribution is less spread and the SHG is more efficient. In all the crystals this region lies in the body of the boule. In Fig. 2 we report the distribution of the domain period of the samples, whose growth parameters are shown in Table 1. Fig. 2 refers to a scan performed over a representative region in the body with a length close to 1 mm. The effective structure period and the corresponding spreading are reported in Table 1. It clearly emerges that the periodic structures with shorter period are less affected by the errors in the border domain position. In particular, the spreading of the period around the mean value is about 8% for the PPLN1 sample while it is of the order of 15% for the PPLN5. This fact suggests that higher pulling and rotational rates are the best conditions to obtain PPLN structures with a sharp domain distribution. Preliminary results indicate that periods shorter than 1.5 μm are difficult to be grown as the coalescence between adjacent domains is easily promoted. This fact is also related to the border domain widths which have a finite value (typically 0.3–0.5 μm [14]). In short period PPLN crystals, the periodically inverted domains only appear in small regions (4 mm × 4 mm) along the boule.Work is in progress to clarify this fact. However, independent of the spreading encountered in the real structure, the presence of errors in the domain boundary position worsens the performance of the PPLN sample in terms of SHG efficiency. The study of the effect of differently sized domains is therefore mandatory to predict the final SHG efficiency.

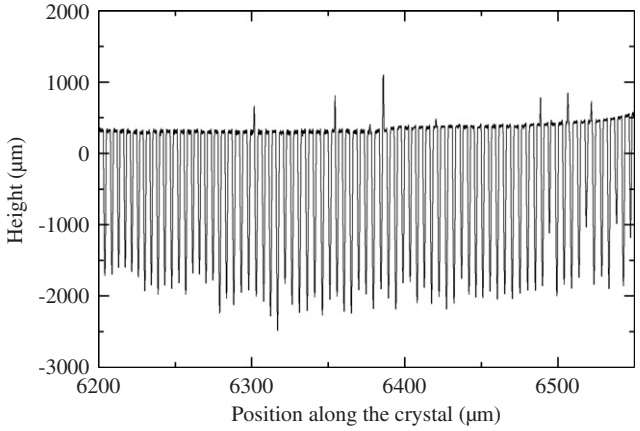


Fig. 1. Profilometer scan of the PPLN structure grown from $Er_2O_3$ = 0.5 mol% with $v_p = 3$ mm/h, $\omega = 12.5$ rpm.

## 4. Second harmonic generation

In this section we will first treat the SHG efficiency expected by a perfect PPLN structure with period equal to the average value given by the profilometer scans. The effect of the border domain errors will consider a further correction.

### 4.1. Second harmonic generation: numerical analysis

In the analysis of the SHG, the type I interaction between a wave $E_1$ at fundamental frequency (FF) $\omega_0$ and

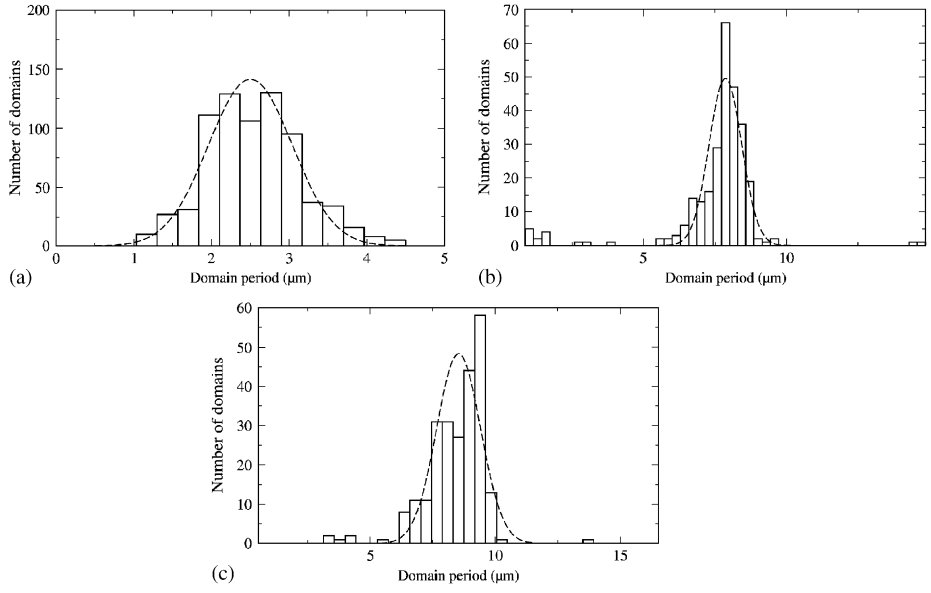


Fig. 2. Domain width distribution relative to (a) PPLN1; (b) PPLN4 and (c) PPLN5 samples. Growth conditions are reported in Table 1. The Gaussian fits were indicated with dashed lines.

a SH wave, $E_2$ at frequency $2\omega_0$, can be described through a set of scalar coupled differential equations. If, in the region of interest, we assume that only the nonlinear interaction between counterpropagating waves is relevant, the following equations hold:

$$\frac{\partial^2 E_1^+(z,y)}{\partial y^2} - 2i\overline{k}\frac{\partial E_1^+(z,y)}{\partial y} + \frac{\partial^2 E_1^+(z,y)}{\partial z^2} + [k_0^2 n^2(\omega_0) - \overline{k}^2]E_1^+(z,y) = -\frac{k_0^2\chi^{(2)}(y)}{\varepsilon_0}[E_1^+(z,y)]^* E_2^-(z,y)\exp(4i\overline{k}y),$$

$$\frac{\partial^2 E_2^-(z,y)}{\partial y^2} + 4i\overline{k}\frac{\partial E_2^-(z,y)}{\partial y} + \frac{\partial^2 E_2^-(z,y)}{\partial z^2} + 4[k_0^2 n^2(2\omega_0) - \overline{k}^2]E_2^-(z,y) = -\frac{2k_0^2\chi^{(2)}(y)}{\varepsilon_0}[E_1^+(z,y)]^2\exp(-4i\overline{k}y), \quad (1)$$

where the "+" and the "−" superscripts refer to FW and BW waves, $\overline{k}$ is the reference wave number and $y$ is the propagation axis.

In the case of forward SHG, similar equations can be easily derived.

In order to evaluate the SHG efficiency, we numerically integrate equations (1) by means of a nonlinear bidirectional beam propagation method (NL Bi BPM) [15,16] already validated and compared with other numerical schemes such as the shooting technique [17]. Since there are no multiple reflections due to linear inhomogeneities along the propagation direction present, a simplified formulation of Bi BPM can be used. Perfectly matched layers (PML) boundary conditions have been chosen to absorb the radiation field [18].

The algorithm adopts a *split-step* technique [19], thus, disjointing the linear part of the problem from the nonlinear one [20] and treating the latter as a perturbation:

$$E_1^+(z,y+\Delta y) = P_1 E_1^+(z,y) + X_1^+,$$
$$E_2^-(z,y) = P_2 E_2^-(z,y+\Delta y) + X_2^-. \quad (2)$$

In Eq. (2) $P_1$ and $P_2$ are the linear propagation operators and the terms $X_1^+$ and $X_2^-$ take into account the nonlinearities. Since these terms are assumed known constants, an iterative procedure is required. So the algorithm implements the following steps:

(1) First the linear problem at the FF must be solved, storing the field propagated in the whole structure; obviously the SH field is zero everywhere.
(2) Then $X$ terms are determined using the previously stored fields and the nonlinear FF and SH problems are solved.
(3) The new values of the FF and the SH fields in the structure are calculated and stored.
(4) If a steady state is reached the procedure is over, otherwise it restarts from point (2).

This numerical method allows to determine FF and SH fields spatial distribution after propagation through a PPLN structure. Initially a perfect periodicity, i.e. without errors in the border domain positions, is assumed. As a further step, these errors will be considered. The mean value of the period measured by the profilometer scan (see Table 2) is used as input in the NL Bi BPM algorithm to predict the ideal SHG efficiency and the SH and FF fields. We analyze the QPM conditions both in the forward and in the backward configurations through the following well-known equation:

$$\Lambda = \frac{\lambda_{FF}}{2(n(2\omega_0) \pm n(\omega_0))}m, \quad (3)$$

where $m$ is the QPM order and the sign "±" refers to the BW (+) and to the FW (−) case. $n(2\omega_0)$, $n(\omega_0)$ are calculated at $T = 20\,^\circ\mathrm{C}$ by means of the Sellmeier equation [21]. We find out that the backward generation can be attained only in the PPLN1 sample; in this case a reasonable BW-QPM order $m$ is feasible provided that an appropriate wavelength is used. In particular, close to $\lambda_{FF} = 1550\,\mathrm{nm}$ we obtain $m = 11$, while FW-SHG is not phase matched.

It is important to underline that in our simulation we neglect the absorption of the $LiNbO_3$ and we assume $|\chi^{(2)}(y)| = 60\,\mathrm{pm/V}$. Fig. 3 shows absolute values of input FW-FF (solid line) and BW-SH (dashed line) electric fields in a structure composed of 250 periods (see also Fig. 4). The pump beam is assumed Gaussian with the peak amplitude equal to $10^7\,\mathrm{V/m}$ and FWHM $= 50\,\mu\mathrm{m}$. Under these hypotheses we predict a SHG efficiency equal to $\eta_{SHG}^{numerical} = 0.02\%$. PPLN4 sample, instead, exhibits FW-SHG efficiency of $\eta_{SHG}^{numerical} = 3.25\%$ for a QPM order

Table 2
Simulations input parameters and resulting efficiency

| Sample | $\lambda$ (nm) | $m$ QPM order | SH | No. layers | $\eta_{SHG}^{numerical}$ (%) | $\eta_{norm,SHG}^{FW/BW}$ (%) | $\eta_{final}$ (%) |
|---|---|---|---|---|---|---|---|
| PPLN1 | 1550 | $m = 11$ | BW | 500 | 0.02 | 2 | 0.001 |
| PPLN4 | 1185 | $m = 1$ | FW | 134 | 3.25 | 6 | 0.195 |
| PPLN5 | 1050 | $m = 1$ | FW | 90 | 4 | 13 | 0.520 |

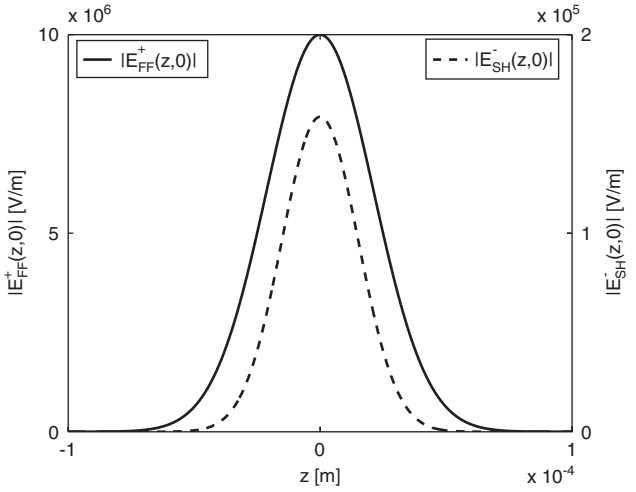


Fig. 3. PPLN1: absolute values of input FW-FF (solid line) and BW-SH (dashed line) electric fields in a structure made of 250 periods. The pump beam is assumed Gaussian with peak amplitude $10^7$ V/m and FWHM = 50 μm.

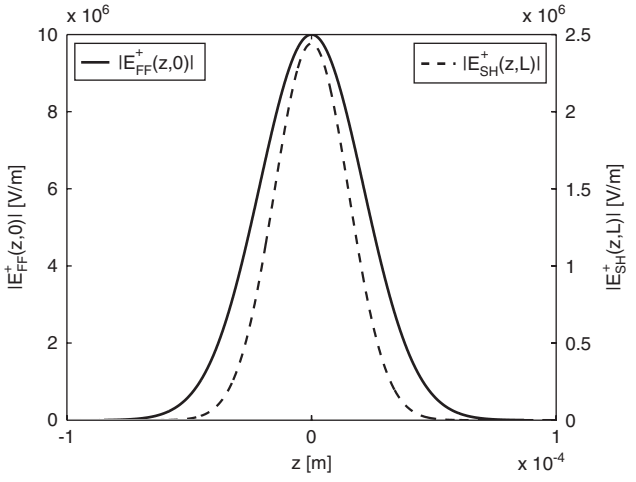


Fig. 4. PPLN4: absolute values of input FW-FF (solid line) and output FW-SH (dashed line) of the electric fields in a structure made of 67 periods.

$m = 1$ at $\lambda_{FF} = 1185$ nm (67 periods length) (Fig. 5). As far as the sample PPLN5 is concerned, its period permits a first-order FW-QPM if the pump wavelength is close to 1050 nm. In Fig. 4 we report the absolute values of input FW-FF (solid line) and output FW-SH (dashed line) electric fields in a structure made of 45 periods. We find out a SHG efficiency close to $\eta_{SHG}^{numerical} = 4\%$. In Table 2 we summarize the simulation parameters and resulting efficiency for all the samples.

### 4.2. Effect of the border domain error on the SHG

When errors in the domain boundary position occur, the phase mismatch at the domain boundaries $\Delta k$ does not coincide with the designed one producing a phase error $\Phi_j$.

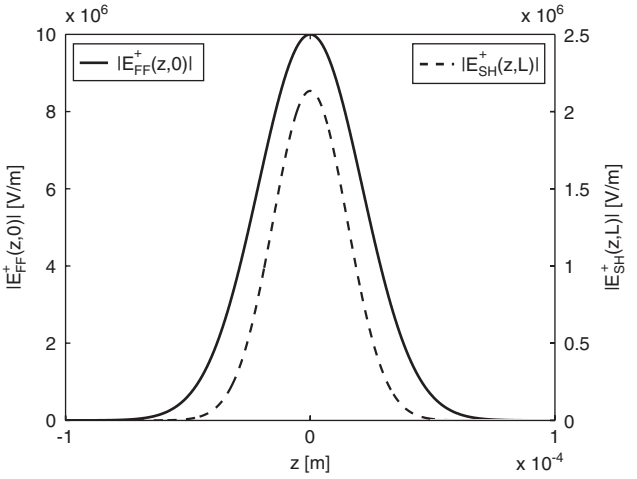


Fig. 5. PPLN5: absolute values of input FW-FF (solid line) and output FW-SH (dashed line) of the electric fields in a structure made of 45 periods.

In particular it results that for the FW SHG:

$$\Phi_j^{FW} = \Delta k \cdot \delta y_j + \delta\Delta k \cdot y_{j,0}, \tag{4}$$

where $y_{j,0} = jmL_c$ is the expected position of the $j$th boundary in the case of a perfect $m$-order QPM condition, $L_c$ being the coherence length. Moreover, $\delta y_j = y_j - y_{j,0}$ is the position error in the $j$th boundary and $\delta\Delta k = \Delta k - \Delta k_0$ represents the deviation of the wave vector mismatch from that at the design point. As reported by Fejer et al. [2], the normalized FW SHG efficiency $\eta_{norm,SHG}^{FW}$ can be expressed in term of the errors in the positions of the domain boundaries as follows:

$$\eta_{norm,SHG}^{FW/BW} = \frac{I_{SHG}}{I_{idealSHG}} = \frac{1}{N^2}\left|\sum_{j=1,\ldots,N} e^{-i\Phi_j^{FW/BW}}\right|^2, \tag{5}$$

where $N$ represents the number of domains, $I_{SHG}$ is the SH intensity expected from the real PPLN structure and $I_{idealSHG}$ is the SH intensity in the case of ideal (i.e. perfect) quasi-phase matching condition. If one focuses the attention on the errors in the domain boundary position and neglects the $\delta\Delta k$ term, $\Phi_j^{FW} = \Delta k \cdot y_j = L_c j - \sum_{i=0}^{j} y_i$ reduces to the accumulated phase error at the $j$th boundary due to its position error. The same equation holds for the backward wave provided that $\Phi_j^{FW}$ is replaced by $\Phi_j^{BW} = (L_c j - \sum_{i=N}^{j} y_i)$. It is worth mentioning that the assumption of neglecting the $\delta\Delta k$ term implies that the efficiency is calculated at a given operating point. By means of Eq. (5) it is, therefore, possible to estimate the normalized FW SHG (or BW SHG, respectively) efficiency expected from real PPLN structure provided that $\delta y_j$ are given. We report in Fig. 6 the value of $\eta_{norm,SHG}^{FW/BW}$ as a function of $\Delta k$ for the various samples while in Table 2 we summarize the maximum value of $\eta_{norm,SHG}^{FW/BW}$. In the case of the FW SHG, the number of periods was chosen to have an equivalent PPLN length close to 1 mm in a crystal region where the period distribution is quite uniform. For the BW case, instead, 250 periods were used to compare the results

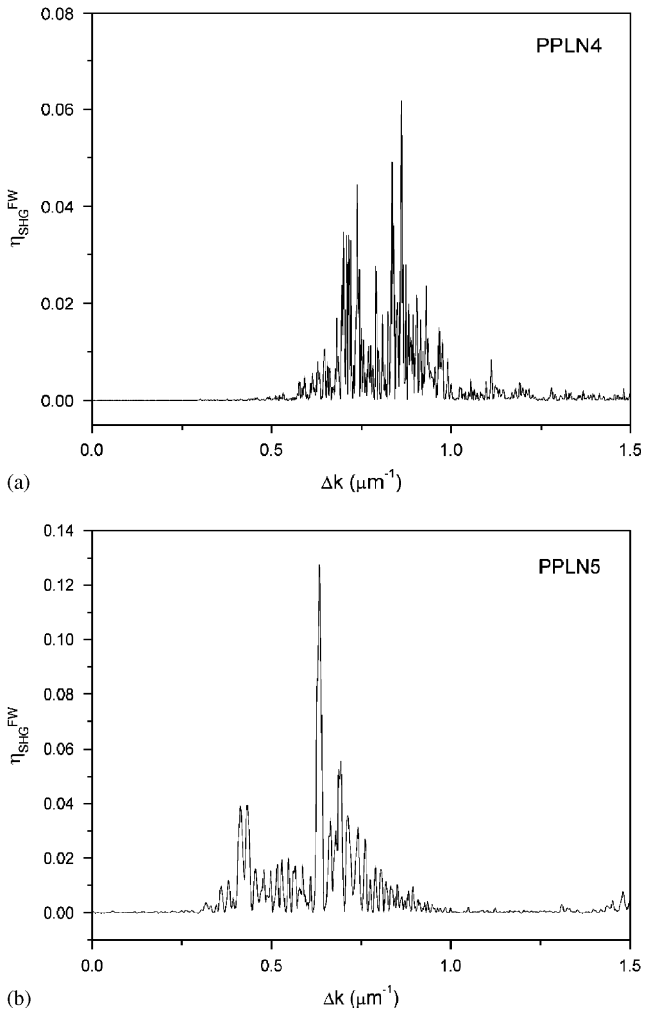


Fig. 6. Normalized SHG conversion efficiency of (a) PPLN4; (b) PPLN5, respectively.

with the numerical analysis. The values of $\eta_{\mathrm{norm,SHG}}^{\mathrm{FW/BW}}$ were calculated at temperature equal to 20 °C, at a fundamental wavelength correspond to the QPM order $m = 1$ for the FW SHG, and $m = 11$ for the BW SHG, respectively. The refractive index value of the medium was the same used in the numerical analysis, i.e. the one given by the Sellmeier equation [21]. From the analysis therefore performed it emerged the maximum FW-SHG efficiency was $\eta_{\mathrm{norm,SHG}}^{\mathrm{FW}} = 13\%$ obtained for the sample PPLN5 at $\Delta k = 0.63\,\mu\mathrm{m}^{-1}$, while for the PPLN4 we found that $\eta_{\mathrm{norm,SHG}}^{\mathrm{FW}} = 6\%$ at $\Delta k = 0.86\,\mu\mathrm{m}^{-1}$.

We underline that the presence of border domain errors introduces satellite peaks in the $\eta_{\mathrm{norm,SHG}}^{\mathrm{FW/BW}}$ plotted versus $\Delta k$. The SHG efficiency predicted by Eq. (5), in fact, is the result of the nonlinear interaction of the fundamental pump light with each subset of domains that present a 'similar' width. In the case of the BW SHG, in the only eligible sample PPLN1 the maximum $\eta_{\mathrm{norm,SHG}}^{\mathrm{BW}}$ was close to 2% at $\Delta k = 3.5\,\mu\mathrm{m}^{-1}$. This result suggests that with proper experimental conditions it is possible to grow a PPLN sample with a period distribution compatible with the BW SHG but for a more efficient BW SHG short periods are needed. Due to the domain coalescence observed in PPLN grown with period shorter than 1.6 μm, the expected final BW SHG is not significant, suggesting that other preparation method should be exploited.

Finally, by means of Eq. (5), one can evaluate how the error in the border domain distribution affects the SHG efficiency. The corrected SHG efficiency is then obtained rescaling $\eta_{\mathrm{SHG}}^{\mathrm{numerical}}$ by the $\eta_{\mathrm{norm,SHG}}^{\mathrm{FW/BW}}$ value calculated at the corresponding $\Delta k$ value. As a consequence, for FW-SHG, the best estimated efficiency is lowered to 0.5% (PPLN5 sample). For BW-SHG, instead, the only sample eligible is the PPLN1 that has a best efficiency close to 0.001%. It is worth mentioning that Eq. (5) predicts a maximum efficiency at the $\Delta k$ value in agreement with Eq. (3).

## 5. Conclusions

In this work we presented the characterization of PPLN structures grown by the off-center Czochralski technique with period ranging from 2 to 10 μm. The study of the domain distribution along the crystal, performed by a profilometer scanning of the etched structures followed by a suitable data processing, allows to check the periodicity of the structure. We observed that at higher rotational rates the PPLN domain distribution is sharper. When higher off-center values are exploited, a period as small as 2 μm can be grown opening the way to interesting applications in terms of BW SHG. To predict the SHG efficiency of the grown periodic structures, we made a spatial analysis of the waves propagating through the PPLN bulk medium by solving the propagation equations through the nonlinear bidirectional beam propagation method. The QPM conditions were applied to both the forward and the backward SHG configurations. While the FW SH wave can be easily matched, we were able to predict the BW SHG only in the sample with the smallest period at the QPM order $m = 11$. Moreover, the errors in the border domain position were taken into account by considering the phase shift induced in the SH wave by the presence of different sized domains and rescaling the SHG efficiency given by the numerical analyses. These analyses allow to test the PPLN samples with period between 2 and 10 μm and to demonstrate that the off-center Czochralski technique is a valid alternative to grow the periodic structures with tailored periods. However, when periods shorter than 1.6 μm are needed other preparation methods are required.

## Acknowledgements

This work has been partially supported by FIRB RBNE01KZ94F and FIRB RBAU01XEEEM.

## References


[1] Armstrong JA, Bloemberger N, Ducuing J, Pershan PS. Interactions between light waves in a nonlinear dielectric. Phys Rev 1962;127:1918–39.

[2] Fejer MM, Magel GA, Jundt DH, Byer RL. quasi-phase-matched second harmonic generation: tuning and tolerances. IEEE J Quantum Electron 1992;28:2631–54.

[3] Russell PSJ. Theoretical study of parametric frequency and wavefront conversion in nonlinear holograms. IEEE J Quantum Electron 1991;27:830–5.

[4] Gu X, Korotkov RY, Ding YJ, Kang JU, Khurgin JB. Backward second-harmonic generation in periodically poled lithium niobate. J Opt Soc Am B 1998;15(5):1561–6.

[5] Ding YJ, Khurgin JB. Backward optical parametric oscillators and amplifiers. IEEE J Quantum Electron 1996;32:1574–82.

[6] Kang JU, Ding YJ, Burns WK, Melinger JS. Backward second-harmonic generation in periodically poled bulk $LiNbO_3$. Opt Lett 1997;22(22):862–4.

[7] Houé M, Townsend PD. An introduction to methods of periodic poling for second-harmonic generation. J Phys D Appl Phys 1995;28:1747–63.

[8] Golenishev-Kutuzov AV, Golenishev-Kutuzov VA, Kalimullin RI. Induced domains and periodic domain structures in electrically and magnetically ordered materials. Phys Usp 2000;43:647–62.

[9] Ming NB, Hong IF, Feng D. The growth of striations and ferroelectric domain structures in Czochrlaski-grown $LiNbO_3$ single crystals. J Mater Sci 1982;17:1663–70.

[10] Argiolas A, Bazzan M, Sada C. A study on the periodicity of periodic poled lithium niobate crystals growth by the off-center Czochralski technique. J Cryst Growth 2003;249:275–82.

[11] Bazzan M, Argiolas N, Bernardi A, Mazzoldi P, Sada C. Topographic investigation of ferroelectric domain structures in periodically-poled lithium niobate crystals by a profilometer. Mat Charact 2003;51:177–84.

[12] Nassau K, Levinstein HJ, Loiacono GM. Ferroelectric lithium niobate. 1. Growth, domain structure, dislocations and etching. J Phys Chem Solids 1996;27:983–8.

[13] Argiolas N, Bazzan M, Bernardi A, Cattaruzza E, Mazzoldi P, Schiavuta P, Sada C, Hangen U, A systematic study of the chemical etching process on periodically poled lithium niobate structures. Mater Sci Eng B 2005;118:150–4.

[14] Cerva BH, Pongratz P, Skalicky P. Lattice defects in single-crystal lithium niobate I. Transmission electron microscopy. Philos Mag A 1986;54:185–97.

[15] Locatelli A, Modotto D, De Angelis C, Pigozzo FM, Capobianco AD. Nonlinear bidirectional beam propagation method based on scattering operators for periodic microstructured waveguides. J Opt Soc Am B 2003;20:1724–31.

[16] Locatelli A, Pigozzo FM, Modotto D, Capobianco AD, De Angelis C. Time-domain BPM for ultrashort pulse propagation in nonlinear multilayers. IEEE Photon Technol Lett 2004;9:2054–6.

[17] Midrio M. Shooting technique for the computation of plane-wave reflection and transmission through one-dimensional nonlinear inhomogeneous dielectric structures. J Opt Soc Am B 2001;18: 1866–71.

[18] Vassallo C, Collino. Highly efficient absorbing boundary conditions for the beam propagation method. J Lightwave Technol 1996;14: 1570–7.

[19] Feit MD, Fleck JA. Light propagation in graded-index optical fibers. Appl Opt 1978;17:3990–8.

[20] Capobianco AD, Brillo D, De Angelis C, Nalesso G. Fast beam propagation method for the analysis of second-order nonlinear phenomena. IEEE Photon Technol Lett 1998;10:543–5.

[21] Schlarb W, Bertzler. Refractive indeces of lithium niobate as a function of wavelength and composition. J Appl Phys 1993;73:3472–7.